Chemistry Europe
European Chemical Societies Publishing

WILEY VCH

Excellence in Chemistry Research

Announcing our new flagship journal

- Gold Open Access
- Publishing charges waived
- Preprints welcome
- Edited by active scientists

Meet the Editors of *ChemistryEurope*

Luisa De Cola
Università degli Studi di Milano Statale, Italy

Ive Hermans
University of Wisconsin-Madison, USA

Ken Tanaka
Tokyo Institute of Technology, Japan

ChemSusChem

Research Article
doi.org/10.1002/cssc.202300613

Chemistry Europe
European Chemical Societies Publishing

www.chemsuschem.org

Robust Light Driven Enzymatic Oxyfunctionalization via Immobilization of Unspecific Peroxygenase

Piera De Santis[+],[a] Deborah Wegstein[+],[b] Bastien O. Burek,*[b] Jacqueline Patzsch,[b] Miguel Alcalde,[c] Wolfgang Kroutil,[d] Jonathan Z. Bloh,*[b] and Selin Kara*[a, e]

Unspecific peroxygenases have attracted interest in synthetic chemistry, especially for the oxidative activation of C–H bonds, as they only require hydrogen peroxide (H_2O_2) instead of a cofactor. Due to their instability in even small amounts of H_2O_2, different strategies like enzyme immobilization or in situ H_2O_2 production have been developed to improve the stability of these enzymes. While most strategies have been studied separately, a combination of photocatalysis with immobilized enzymes was only recently reported. To show the advantages and limiting factors of immobilized enzyme in a photobiocatalytic reaction, a comparison is made between free and immobilized enzymes. Adjustment of critical parameters such as (i) enzyme and substrate concentration, (ii) illumination wavelength and (iii) light intensity results in significantly increased enzyme stabilities of the immobilized variant. Moreover, under optimized conditions a turnover number of 334,500 was reached.

Introduction

In the 1990s, the advent of *Green Chemistry* marked an epoch-making change in scientists' and researchers' perspectives worldwide regarding how they used to design new molecules and their synthetic pathways. It was for the first time that economic profits and product yields stopped being the only evaluation parameters for the excellent rating of a synthetic process. This is how atom economy, prevention, and use of renewable feedstocks soon became crucial criteria in chemical processes at both laboratory and industrial levels. Moreover, such a revitalized chemical research shift paves the way for new research fields and their application on a manufactory scale. Among them, a position of honor is occupied by biocatalysis. Although researchers have always employed enzymes, it is only in the latest decades that it has become a right and extensively used approach for chemical synthesis. Biocatalysis, taking advantage of nature's arsenal of catalysts, not only offers new solutions to overcome the limits of some traditional chemical processes, but it also enhances the development of greener and sustainable processes.[1] In addition, relatively new strategies such as protein engineering, enzyme immobilization, online analysis, and in situ product removal, enable biocatalysts to meet the strict process conditions often occurring in industry.[2] A perfect illustration for this is the selective oxyfunctionalization of C–H, C–C and C=C bonds, which represents a crucial step in several industrial processes. Traditional approaches rely on transition metal catalysts, potent oxidant/reductant agents, and severe conditions negatively affecting human health and the environment.[3] Besides all these disadvantages, it is also essential to highlight the mediocre regio- and stereo-selectivity of these synthetical routes.

Conversely, different enzymes catalyzing oxyfunctionalization reactions can be found in nature, and among them, particular attention has been given to unspecific peroxygenases (UPOs, EC 1.11.2.1).[4] This enzyme superfamily presents several advantages if compared to other similar biocatalysts; first of all, their self-sufficiency from expensive cofactors. In fact, even though UPOs are heme-thiolate enzymes like the well-known P450 monooxygenases, they are independent from the use of

[a] *P. De Santis,[+] Prof. Dr. S. Kara*
Biocatalysis and Bioprocessing Group, Department of Biological and Chemical Engineering
Aarhus University
Gustav Wieds Vej 10, 8000 Aarhus C (Denmark)
E-mail: selin.kara@bce.au.dk

[b] *D. Wegstein,[+] Dr. B. O. Burek, J. Patzsch, Dr. J. Z. Bloh*
DECHEMA-Forschungsinstitut
Theodor-Heuss-Allee 25, 60486 Frankfurt am Main (Germany)
E-mail: bastien.burek@dechema.de
jonathan.bloh@dechema.de

[c] *Prof. Dr. M. Alcalde*
Department of Biocatalysis
Institute of Catalysis
ICP CSIC, C/ Marie Curie 2, 28049 Madrid (Spain)

[d] *Prof. Dr. W. Kroutil*
Field of Excellence BioHealt, BioTechMed, Institute of Chemistry
University of Graz
Heinrichstrasse 28, 8010 Graz (Austria)

[e] *Prof. Dr. S. Kara*
Institute of Technical Chemistry
Leibniz University Hannover
Callinstr. 5, 30167 Hannover (Germany)
E-mail: selin.kara@iftc.uni-hannover.de

[+] *These authors contributed equally to this work.*

Supporting information for this article is available on the WWW under https://doi.org/10.1002/cssc.202300613

expensive electron donors like nicotinamide adenine dinucleotide phosphate (NADPH) and auxiliary flavoproteins. Conversely, they rely on H_2O_2 as an oxidation agent to fulfill their catalytic route.[5] In addition, UPOs benefit from higher turnover numbers, a broad substrate scope as well as increased stability.[6] In particular, the UPO from the edible mushroom *Agrocybe aegerita* and its evolved mutant variant PaDa-I have been the subject of several investigations.[4c,7] However, despite their unquestioned potential, the application of UPOs at the industrial scale is still hindered by limitations like cost-effective production and sensitivity towards H_2O_2.[8] As far as the former is concerned, enzyme immobilization is a widely-recognized technique with beneficial effects on different issues. This strategy not only helps improving enzyme stability in different organic solvents (also at extreme values of pH and temperature) but also enables their recyclability and simplifies downstream processing.[9] All these advantages play a crucial role in developing a biocatalyst with an increased catalytic performance fitting the industrial requirements.[10,11] After an in-depth study of different carrier-bound and carrier free methods, a proper immobilization procedure has been developed and optimized for the PaDa-I variant. The enzyme has been successfully immobilized on an amino carrier via covalent binding obtained through a simple carbonylamine condensation reaction, reaching an immobilization yield of 55% and a 15-fold higher half-life time.[12] Further studies proved the applicability of the developed procedure in both rotating bed reactors and continuous flow system.[13] When it comes to H_2O_2-mediated deactivation issues, they can be elegantly mitigated via in situ production. In the last years, several approaches have been developed for this purpose.[14] This strategy allows a gradual *in situ* supply of the oxidant, maintaining its concentration at a non-harmful level. Using a photocatalyst for the H_2O_2 provision proved to be a very up and coming and eco-friendly option.[15] In this context, the wise combination of UPO with photocatalysts such as flavin adenine mononucleotide (FMN), titanium dioxide, carbon nanodots (CNDs), and graphitic carbon nitride (g-C_3N_4) led to interesting results: high turnover number (TON) increased enzyme stability as well as good product selectivity.[14b,16] Moreover, it has been demonstrated that even better results could be obtained by adding sacrificial electron donors like methanol.[17]

Our current study aims to further optimize the PaDa-I catalytic performance by combining the advantages of enzyme immobilization with the ones related to the photocatalytic in situ H_2O_2 generation. To the best of our knowledge, although it is the first time this union has been proposed, it promises to be a practical approach to overcoming the limitations of UPOs. In a similar approach, UPO was immobilized directly on palladium-loaded titanium dioxide. Chiral alcohols such as hydroxyethylbenzene were obtained with high selectivities and better conversion rates than with free enzyme.[18] In our study, the enzyme and photocatalyst are intentionally separated to allow for greater flexibility, i.e., for example, it is possible to change the photocatalyst without having to adjust the method of enzyme immobilization, and it allows for better matching of the amount of photocatalyst and enzyme.

Results and Discussion

The generally higher stability of immobilized UPO,[12] and the possibility for spatial separation of photocatalyst and enzyme should minimize enzyme deactivation in a photoenzymatic system and therefore can lead to higher enzymatic turnovers. To prove this, we combined the covalently immobilized PaDa-I on the most promising amino methacrylate carrier (ECR8315F) with a potassium phosphate-modified graphitic carbon nitride (g-C_3N_4), which is known to produce H_2O_2 efficiently under UV and visible light illumination.[19] As a model reaction, we investigated the oxyfunctionalization of 4-ethylbenzoic-acid (EBA) shown in Scheme 1.

In the first step the enzyme uses the in situ photocatalytically produced H_2O_2 to hydroxylate EBA to 4-(1-hydroxyethyl) benzoic acid (HEBA), which can be further oxidized to 4-acetylbenzoic acid (ABA). The enzyme's activity towards this overoxidation reaction is almost negligible, which we assessed in a separate experiment without photocatalyst and manual H_2O_2 addition (see SI Figure S18). Conversely, the photocatalyst can catalyze either the overoxidation step or the direct oxidation from EBA to ABA, depending on its nature and illumination conditions.[20] However, under the conditions applied herein the g-C_3N_4 showed a very low activity to convert EBA into ABA (see SI Figure S16). Compared to the more often used hydroxylation of ethyl benzene, EBA is readily soluble in aqueous media (in our case of 10 vol.% methanol in 0.1 M phosphate buffer the solubility is at least 50 mM, while the solubility for ethyl benzene is approx. 1.5 mM), which allows for closing the mass balance and calculating a selectivity [$S = mole_{HEBA}/(mole_{HEBA} + mole_{ABA})$]. For the photoenzymatic reactions we used methanol as an electron donor as it is established that this improves H_2O_2 production and enzyme stability.[14b,16a]

As the immobilization yield of PaDa-I on this carrier is 55%, but the activity yield is only 2%,[12] it is difficult to directly compare it with the free enzyme. Thus, we decided to make the comparison based on the amount of crude enzyme used for immobilization, which means that the turnover number ($TON = mole_{product}/mole_{enzyme}$) of the active immobilized enzyme is highly underestimated. Consequently, all concentrations stated in this manuscript for the immobilized enzyme refer to the amount of free enzyme used in the immobilization procedure. From an application point of view, this should be the most reasonable way to compare the systems, as it is essential to

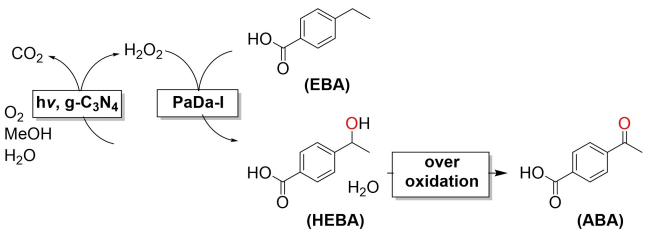

Scheme 1. Schematic representation of the cascade reaction. Photocatalytic in situ production of H_2O_2 to drive the enzymatic conversion of 4-ethylbenzoic acid (EBA) to 4-(−1-hydroxyethyl) benzoic acid (HEBA) and its possible oxidation to 4-acetylbenzoic acid (ABA).

know how much product can be formed out of the initially used enzyme. However, if the immobilization yield can be further improved, the TON for the immobilized enzyme gets even more advantageous. A comparison of the concentration-time profiles for the photobiocatalytic cascade with free and immobilized UPO is shown in Figure 1.

At the beginning of the reaction, a linear increase in product formation can be observed for both enzyme formulations. For the free enzyme, the product formation stops after approx. 1.5 h while the immobilized enzyme is active for at least 4 h. In both cases ABA can be observed, mainly generated by the photocatalytic oxidation of HEBA as the enzyme shows almost no activity for this reaction (see SI Figures S17 and S18). The stop of an increase of the sum of both products indicates that the enzyme is inactivated because adding freshly prepared enzyme leads to a renewed increase in product concentration, as shown in SI Figure S6.

This first experiment already proved that the immobilized enzyme is slightly more stable in the photobiocatalytic system compared to the free enzyme, leading to a 15% higher TON.

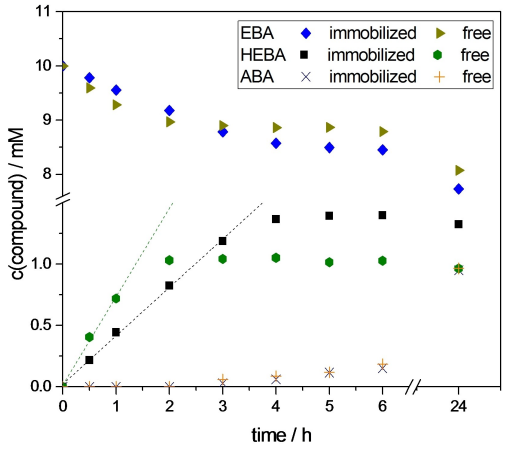

Figure 1. Comparison of the concentration-time profiles of the photobiocatalytic cascade of immobilized and free enzyme for the conversion of 4-ehtylbenzoic acid (EBA) to 4-(1-hydroxyl ethyl) benzoic acid (HEBA) and 4-acetylbenzoic acid (ABA). Reaction conditions: 10 mM EBA, 2 g L^{-1} g-C_3N_4 and 20 nM enzyme in 0.1 M phosphate buffer with a pH of 7 containing 10 vol% methanol, at 365 nm and 544 µE L^{-1} min^{-1}, 25 °C and 2 mL min^{-1} O_2-bubbling.

The free enzyme has a 27% higher initial product formation rate and therefore also a higher H_2O_2 efficiency (see SI for H_2O_2 production data) indicating kinetic limitations of the immobilized enzyme. The H_2O_2 efficiency can be expressed as the quotient of the product formation rate in the photobiocatalytic system, and the rate of H_2O_2 produced in the system measured without enzyme (EFF of $H_2O_2 = r_{product}/r_{H2O2}$). The EFF indicates how well the photocatalytic H_2O_2 synthesis matches the enzyme's specific consumption. As H_2O_2 in excess leads to an inactivation of the enzyme a high EFF is vital to prevent the accumulation of H_2O_2. To exclude the carrier influences on the slow product formation, for example, by shading part of the light from the photocatalyst and thereby leading to lower H_2O_2 formation, we examined its light absorption behavior by diffuse reflection spectroscopy. The corresponding Kubelka-Munk-plot (cf. SI Figure S20) showed only a small absorption band below 350 nm, but no absorption in the visible range, which is consistent with the white color of the carrier. Furthermore, photocatalytic oxygen reduction experiments with the pure carrier without enzymes showed no difference in H_2O_2 formation (see Figure S15).

As the H_2O_2 formation is equal in both enzymatic cases, we wanted to analyze the kinetic limitations of the immobilized enzyme. We varied the enzyme concentration from 10 to 100 nM and the substrate concentration from 1 to 50 mM. The respective turnover number, initial product formation rate, selectivity, and H_2O_2 efficiency are shown in Figure 2.

Increasing the enzyme concentration first leads to a rise in the product generation rate, which hardly further increases at above 40 nM. The optimal conditions for achieving high enzymatic turnovers range from 20 to 40 nM. In fact, at higher enzyme concentrations, even if the final product concentration (and the overoxidation product ABA) increases, the enlarged amount of enzyme keeps the TON values low. Also, the turnover frequency (TOF = r_{HEBA}/c_{enzyme}) is constant for the first two enzyme concentrations with approx. 9.1 s^{-1} and decreases at higher enzyme concentrations down to 3.7 s^{-1}. Probably the reaction is limited by H_2O_2 or substrate, so part of the enzyme is unproductive and only degrades. Conversely, it is essential to highlight that the variation in enzyme concentration did not strongly affect product selectivity.

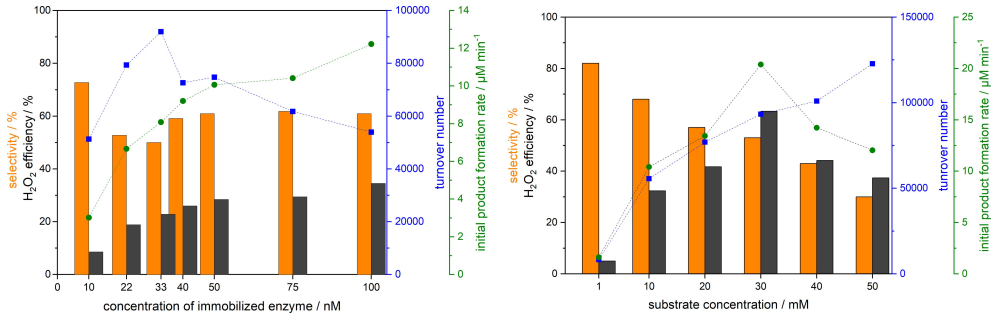

Figure 2. Impact of the variation of the enzyme concentration (left) and substrate concentration (right) on turnover number (blue), initial product formation rate (green), selectivity (orange) and H_2O_2 efficiency (black). Reaction conditions: 2 g L^{-1} g-C_3N_4 in 0.1 M phosphate buffer with a pH of 7 containing 10 vol% methanol, at 365 nm and 544 µE L^{-1} min^{-1}, 25 °C, 2 mL min^{-1} O_2-bubbling and 10 mM EBA (left) and 75 nM UPO (right). Selectivity = $mole_{HEBA}/(mole_{HEBA} + mole_{ABA})$; EFF = $r_{product}/r_{H2O2}$.

To investigate the influence of the substrate concentration, we kept the photon flux (q_p) constant and chose a high enzyme concentration of 75 nM, since limitations in productivity were evident with 10 mM of substrate. Decreasing the EBA concentration down to 1 mM dramatically decreased the reaction rate. Even if the conversion with 62% and selectivity with 82% were higher, the TON was very low. On the one hand this is intrinsic due to the low substrate concentration which makes it impossible to reach a TON higher than 50,000. On the other hand, the low H_2O_2 efficiency leads to an accumulation that is harmful to the enzyme. Interestingly, in all cases, the enzyme is inactivated approximately after 5–6 h, indicating that H_2O_2 may not be the leading cause of enzyme inactivation under these conditions. Raising the substrate concentration first leads to a faster product formation which reaches an optimum at around 30 mM (with a TOF of 8.1 s^{-1}), while at higher substrate concentrations the speed of the reaction decreases again. This can be explained by substrate inhibition, which was already observed for this substrate for the free enzyme and is a known effect in ping-pong mechanism-based systems.[14a] At 30 mM also, the highest apparent quantum yield (AQY $= r_{product} \times 2/q_p$, as two photons are required per turnover) of 7.5% has been reached. Even though it was not our goal to optimize this, it is an acceptable utilization of photons compared to many other systems with AQYs typically below 1%.[20] The TON increases over the whole investigated range; however, above 30 mM it is mainly driven by the more pronounced overoxidation. Therefore, the selectivity decreases linearly with an increasing substrate concentration.

Both graphs highlight how important it is to balance the photo- and the enzyme catalysis, as even small changes impact the overall performance. This gets even clearer if one looks closely at the photocatalysis side of the cascade. Since the reaction is highly dependent on H_2O_2, it is evident that an adjustment of its formation is necessary to optimize the system. Amongst other reaction parameters, the H_2O_2 production rate directly responds to the light intensity and excitation wavelength.[19,21] As the g-C_3N_4 used has a band gap of about 2.8 eV (cf. Figure S22) it can be excited with wavelengths up to about 450 nm (blue light).[19] Therefore, we evaluated the impact of four wavelengths ranging from 365 nm over 385 nm and 415 nm to 450 nm (Figure 3).

To determine the influence of H_2O_2, first the photocatalytic formation of H_2O_2 was investigated without enzyme under the same conditions (cf. Figure 3, left). At 365 and 385 nm, H_2O_2 formation was about the same, but with 415 nm excitation only a third, and at 450 nm only 2.5% of that. H_2O_2 also influences the product formation rate, which decreases significantly as the wavelength increases, but in a different ratio. While at 450 nm the formation decreases by a factor of 20 compared to 365 nm, at 415 nm it is only half as small. This is also visible in the H_2O_2 efficiency which increases with a lower H_2O_2 formation rate. Also, a higher enzymatic stability is achieved at a higher wavelength.

It was noticeable that the TON at 365 nm was much higher than in the previous experiments. The only difference was that we used another set-up for the illumination with different wavelengths; all other parameters like the incident photon flux have been kept constant. The previously shown results have been obtained in a reactor illuminated from the side, while for the wavelength variation the illumination was from below as shown in Figures S1 and S2. To find a comprehensible explanation, we investigated the light-mediated inactivation of the enzyme, as we knew that the free enzyme can be deactivated just by shining light on it.[17] Unexpectedly, the immobilized enzyme loses its activity even more rapidly under light exposure than the free enzyme. Comparable to the free enzyme, the inactivation slows with increasing wavelength (see SI Figure S19). As the photocatalyst is not perfectly dispersed in this reactor, which leads to slightly higher catalyst concentrations in the lower region of the reactor, the photocatalyst has a higher shadowing effect with bottom illumination, which protects the enzyme from direct light inactivation. Thus, illumination from the bottom leads to higher enzyme stabilities in this case.

All reactions showed a relatively poor selectivity below 60%. Therefore, it appeared conclusive to lower the light intensity to reduce the photocatalytic oxidation of HEBA to ABA and slow down enzyme inactivation. We performed the same set of experiments again with half of the light intensity (225 µE L^{-1} min^{-1} instead of 544 µE L^{-1} min^{-1}). Indeed, the

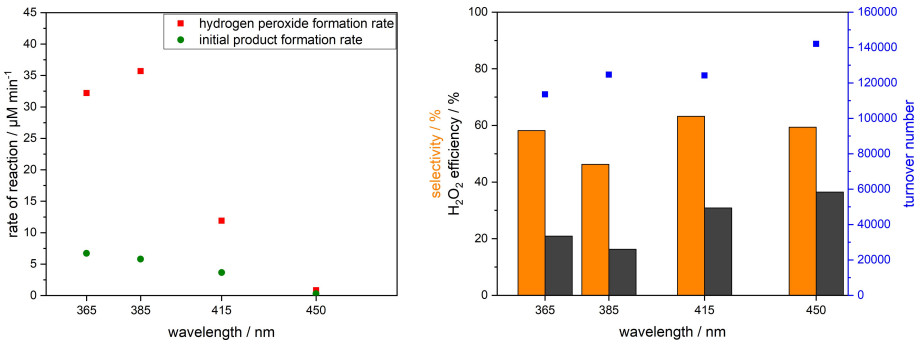

Figure 3. Comparison of different illumination wavelengths at the same volumetric photon flux of 544 µE L^{-1} min^{-1}. On the left side H_2O_2 (red) and product (green) formation, and on the right respective selectivity (orange), H_2O_2 efficiency (black) and turnover number (blue). Reaction conditions: 10 mM EBA, 2 g L^{-1} g-C_3N_4 and 20 nM enzyme in 0.1 M phosphate buffer with a pH of 7 containing 10 vol% methanol, at 544 µE L^{-1} min^{-1}, 25 °C and 2 mL min^{-1} O_2-bubbling.

selectivity could be improved for all reactions and the slower enzyme inactivation led to higher TON at 365, 385 and 415 nm. As seen from Figure 4, halving the light intensity also leads to an approximate halving of the H_2O_2 production rate. However, the product formation rates decrease by less than that in all cases, which leads to higher H_2O_2 efficiencies. This is a general trend, the lower the photocatalytic H_2O_2 production, the higher the H_2O_2 efficiency. However, the results emphasize that H_2O_2 plays a rather subordinate role in enzyme inactivation under these conditions as the highest TON was reached at 415 nm, which has neither the lowest H_2O_2 production nor the highest H_2O_2 efficiency. Furthermore, lowering the light intensity and H_2O_2 formation in the case of 450 nm led to a lower TON, even though the H_2O_2 efficiency increased significantly.

Since our goal was to show that the immobilized enzyme can be more stable than the free enzyme in the photo-enzymatic system, we performed enzyme reactions with 20 nM non-immobilized enzyme under the same conditions and compared the TON. As seen in Figure 5 on the left, the TON are similar, with a slight stability advantage at 365 nm and 385 nm for the immobilized enzyme, but at 415 nm the free enzyme performed slightly better. Only at 450 nm can it be seen that the immobilized enzyme produces a significantly higher turnover and is stable in the reaction over several days. This shows that the optimal conditions for high enzymatic turnovers differ in case of free and immobilized enzymes. However, this comparison is still based on the assumption of the enzyme concentration used for immobilization. Considering that the immobilization yield is about 55%, the real concentration of the immobilized enzyme in the reactions is only 11 nM. To compare the amount of enzyme within the reaction we also performed the same reactions with 10 nM of the free enzyme (see SI Figure S11). With 10 nM free enzyme significantly higher TTNs at all wavelengths could be observed compared to 20 nM of free enzyme (cf. Figure 5). The immobilized enzyme, however, showed even 20–37% higher turnover numbers for 415 nm, 385 nm, and 365 nm. Under blue light illumination, the TON of immobilized enzyme was even 2.5 times higher than with free enzyme. This again highlights the need to improve the immobilization yield further to fully exploit the advantages of the immobilized enzyme from a user's perspective.

As expected, the free enzyme showed a higher product formation rate and, thus TOF and H_2O_2 efficiency. However, the relatively low TOF of 9.2 s^{-1} at best, which is only 33% higher compared to immobilized enzyme, indicates that the free enzyme is highly limited by H_2O_2, as the TOF can be up to 40 times higher under ideal EBA and H_2O_2 concentrations.[14a] Surprisingly, a higher selectivity to HEBA was achieved with

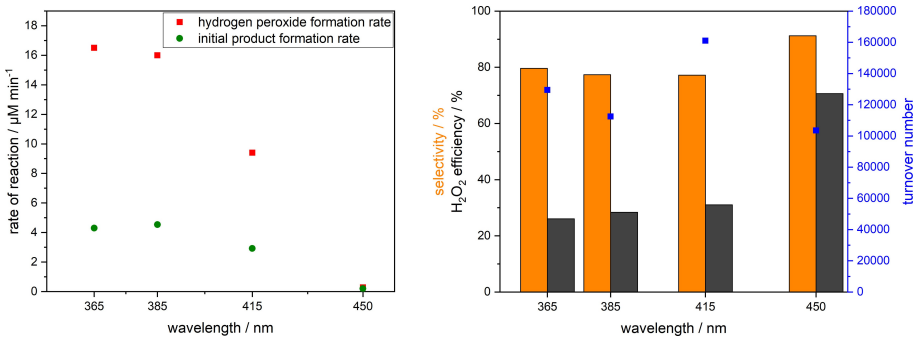

Figure 4. Comparison of different illumination wavelengths at the same volumetric photon flux of 225 µE L^{-1} min^{-1}. On the left side H_2O_2 (red) and product (green) formation, and on the right respective selectivity (orange), H_2O_2 efficiency (black) and turnover number (blue). Reaction conditions: 10 mM EBA, 2 g L^{-1} g-C_3N_4 and 20 nM enzyme in 0.1 M phosphate buffer with a pH of 7 containing 10 vol% methanol, at 225 µE L^{-1} min^{-1}, 25 °C and 2 mL min^{-1} O_2-bubbling.

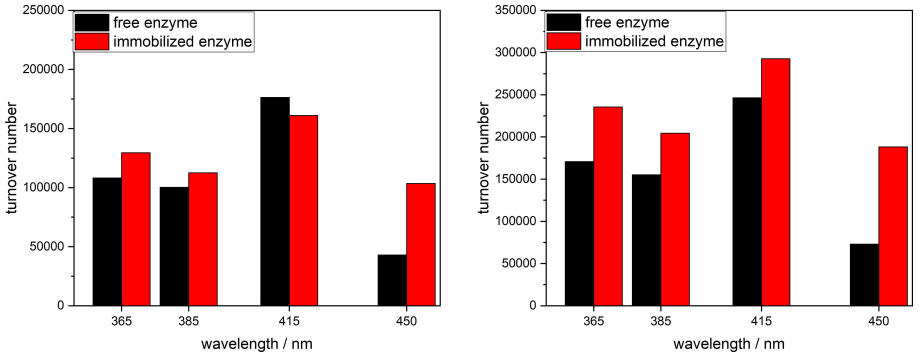

Figure 5. Comparison of total turnover numbers of free (black) and immobilized (red) enzyme under variation of the excitation wavelength. On the left the comparison is based on the enzyme amount used for immobilization which corresponds to 20 nM, therefore compared to 20 nM of free enzyme. On the right the comparison is based on the amount of enzyme within the reaction which is 11 nM due to 55% immobilization yield, compared to 10 nM of free enzyme. Reaction conditions. 10 mM EBA, 2 g L^{-1} g-C_3N_4 in 0.1 M phosphate buffer with a pH of 7 containing 10 vol% methanol, at 225 µE L^{-1} min^{-1}, 25 °C and 2 mL min^{-1} O_2-bubbling.

immobilized enzyme, which was only around 60% with the free enzyme. In comparison, it ranged around 80% for the immobilized enzyme (see SI Table S2 for more specific reaction details).

According to the collected results, one last photoreaction was performed by combining all the optimal conditions to reach a high turnover number with the immobilized enzyme. Using a low light intensity (225 $\mu E\,L^{-1}\,min^{-1}$) under violet illumination (415 nm) and 30 mM of substrate together with 30 nM enzyme, a satisfying turnover number of 184,000 (corresponding to 16.5 nM enzyme within the reaction, respectively, a TON of 334,500) could be achieved.

Conclusions

Overall, we have investigated the use of immobilized unspecific peroxygenase variant PaDa-I from *Agrocybe aegerita* (*Aae*UPO) on an amino carrier in a photobiocatalytic oxyfunctionalization process using g-C_3N_4 as a photocatalyst for in situ H_2O_2 supply. The immobilized enzyme shows generally higher stability compared to the free enzyme. However, the optimal reaction conditions differ for the two enzyme variants, which is why the stability advantage of the immobilized enzyme is pronounced differently. The most significant advantage with up to 250% higher enzymatic turnover was shown under illumination with blue light (450 nm). Under optimized conditions a very promising turnover number of 334,500 for the immobilized enzyme inside the reaction (corresponding to 184,000 turnovers considering the enzyme quantity used for immobilization) could be reached. Since inactivation by light is so pronounced with this carrier further efforts will focus on alternative carrier materials optimizing the enzyme stability against light. Furthermore, current trends in the design of new photocatalysts, e.g., s-schemes,[22] will be evaluated for H_2O_2 generation and improved compatibility with the enzyme in the future.

Experimental Section

General information

All solvents, reactants, and starting materials were received from commercial suppliers in the highest available purity (Sigma Aldrich, VWR, Carl Roth, Thermo Fisher) and used as received. Ultrapure water was produced with a MilliQ® synthesis system by Merck Millipore (Darmstadt, Germany). All experiments were carried out under atmospheric conditions if not stated otherwise. The mutant variant *Aae*UPO PaDa-I was produced *via* fermentation as described by Hobisch et al.[23] For photometric measurements, a temperature-controlled Cary 60 UV-Vis spectrophotometer from Agilent technologies (Santa Clara, California, United States) was used.

Enzyme immobilization

The enzyme was covalently immobilized on the amino carrier Lifetech™ ECR8315F from Purolite Life Sciences Ltd. (Llantrisant, United Kingdom) as detailed reported by De Santis et al.[12] and then characterized via Bicinchoninic acid protein assay (Pierce™ 660 nm) and ABTS (2,2′-azino-bis(3-ethylbenzothiazoline-6-sulfonic acid)) activity assay.[24] Moreover, the activity assay was systematically repeated to track the enzyme activity throughout the whole study.

Enzyme activity assay

UPO relative activity was determined using the oxidation of ABTS to its green radical which can be analyzed via UV-Vis ($\lambda = 405$ nm). A mixture of 14.5 µL H_2O_2 (3.5%) and 10 mL ABTS (0.3 mM) in citrate/phosphate buffer (0.1 M, pH 4.4) were added to 300 µL of the reactor solution from the reaction mixture. Samples were taken every 30 to 60 seconds and the enzyme was removed using a syringe filter. 200 µL of these samples were pipetted into a microtiter plate and the absorbance was measured in a microplate reader (PowerWave HT, BioTek).

Photocatalyst preparation

To synthesize graphitic carbon nitride with intercalated potassium and phosphate ions, 4 g of melamine and 7.5 mmol of K_2HPO_4 was calcined for 4 h at 550 °C (2.2 $K\,min^{-1}$ heating rate) in a porcelain cup covered with a cap.[19] After grinding the resulting powder in a mortar, a suspension (2 $g\,L^{-1}$) of the photocatalyst was prepared in potassium phosphate buffer (0.1 M, pH 7) and treated with ultrasound (Emmi-H30 ultrasonic bath from EMAG, 180 W, 3 h) to obtain a more stable suspension.

Photoreactions

The photoreactions were all performed with 4-ethylbenzoic acid as model substrate, and as previously mentioned, its initial concentration in the reactor varied from 1 to 50 mM. The covalently immobilized enzyme (from 10 to 100 nM) was incubated with 2 $g\,L^{-1}$ of g-C_3N_4 in phosphate buffer (100 mM pH 7) with 10% methanol as an electron donor. Moreover, the reactors were exposed to different light intensities and wavelengths at 25 °C and 500 rpm. Samples were collected regularly and analyzed via HPLC analysis.

Analytics

Conversion of all reactions was measured via HPLC with a Nexera X2 from Shimadzu with a reverse phase column ACQUITY UPLC BEH C18 from Waters. A gradient of acetonitrile and water with 0.1 volume percent formic acid was used as eluent. The flow rate was 1.2 $mL\,min^{-1}$ with an injection volume of 1 µL. During elution, the first 30 seconds were eluted with ratio of 90:10 (water:acetonitrile). Then, a ratio of 5:95 was set over a period of 70 seconds, which was maintained for 80 seconds. Lastly, the ratio was changed to the starting value of 90:10 within one minute, resulting in a total elution time of 4 minutes. The column temperature was 50 °C during the entire time. Analytes were detected using a SPDM20 A UV/Vis detector (Shimadzu) at 237 nm by comparison to a calibration between 0.1 and 3 mM with the substrate and both products in potassium buffer.

Acknowledgements

S.K. acknowledges Independent Research Fund Denmark (PHOTOX-*f* project, grant No 9063-00031B) for the grant funding in the framework of Sapere Aude DFF Starting Grant. This project

has received funding from the European Union's Horizon 2020 research and innovation program under the Marie Skłodowska-Curie grant agreement No 764920. Deutsche Forschungsgemeinschaft (DFG) under funding code BL 1425/1-2 is gratefully acknowledged.

Conflict of Interests

The authors declare no conflict of interest.

Data Availability Statement

The data that support the findings of this study are available from the corresponding author upon reasonable request.

Keywords: photocatalysis · biocatalysis · peroxygenases · g-C_3N_4 · immobilized enzyme

[1] a) S. Wu, R. Snajdrova, J. C. Moore, K. Baldenius, U. T. Bornscheuer, *Angew. Chem. Int. Ed.* **2021**, *60*, 88–119; b) R. A. Sheldon, J. M. Woodley, *Chem. Rev.* **2018**, *118*, 801–838.
[2] a) J. M. Woodley, *Appl. Microbiol. Biotechnol.* **2019**, *103*, 4733–4739; b) P. De Santis, L.-E. Meyer, S. Kara, *React. Chem. Eng.* **2020**, *5*, 2155–2184.
[3] a) H. K. P. Reddy, *J. Mol. Catal. A: Chem.* **2012**, *335*, 180–185; b) J. B. Cohen, *A Class Book Of Organic Chemistry*, Macmillan and Co., Limited, London, **1919**; c) T. Harada, K. Kanda, *Org. Lett.* **2006**, *8*, 3817–3819.
[4] a) S. Bormann, A. G. Baraibar, Y. Ni, D. Holtmann, F. Hollmann, *Catal. Sci. Technol.* **2015**, *5*, 2038–2052; b) Y. Wang, D. Lan, R. Durrani, F. Hollmann, *Curr. Opin. Chem. Biol.* **2017**, *37*, 1–9; c) M. Hofrichter, R. Ullrich, *Curr. Opin. Chem. Biol.* **2014**, *19*, 116–125.
[5] a) S. Chakrabarty, Y. Wang, J. C. Perkins, A. R. H. Narayan, *Chem. Soc. Rev.* **2020**, *49*, 8137–8155; b) M. Ramirez-Escudero, P. Molina-Espeja, P. Gomez de Santos, M. Hofrichter, J. Sanz-Aparicio, M. Alcalde, *ACS Chem. Biol.* **2018**, *13*, 3259–3268; c) S. Kara, J. H. Schrittwieser, F. Hollmann, M. B. Ansorge-Schumacher, *Appl. Microbiol. Biotechnol.* **2014**, *98*, 1517–1529.
[6] a) J. Dong, E. Fernandez-Fueyo, F. Hollmann, C. E. Paul, M. Pesic, S. Schmidt, Y. Wang, S. Younes, W. Zhang, *Angew. Chem. Int. Ed.* **2018**, *57*, 9238–9261; b) G. Grogan, *JACS Au* **2021**, *1*, 1312–1329.
[7] a) M. C. R. Rauch, F. Tieves, C. E. Paul, I. W. C. E. Arends, M. Alcalde, F. Hollmann, *ChemCatChem* **2019**, *11*, 4519–4523; b) M. Hofrichter, H. Kellner, R. Herzog, A. Karich, C. Liers, K. Scheibner, V. Kimani, R. Ullrich, *Fungal Peroxygenases: A Phylogenetically Old Superfamily of Heme Enzymes with Promiscuity for Oxygen Transfer Reactions*, Springer, Cham, **2020**, pp 369–403; c) P. Molina-Espeja, E. Garcia-Ruiz, D. Gonzalez-Perez, R. Ullrich, M. Hofrichter, M. Alcalde, *Appl. Environ. Microbiol.* **2014**, *80*, 3496–3507; d) P. Molina-Espeja, S. Ma, D. M. Mate, R. Ludwig, M. Alcalde, *Enzyme Microb. Technol.* **2015**, *73–74*, 29–33.
[8] a) A. Karich, K. Scheibner, R. Ullrich, M. Hofrichter, *J. Mol. Catal. B: Enzym.* **2016**, *134*, 238–246; b) X. Wang, R. Ullrich, M. Hofrichter, J. T. Groves, *Proc. Natl. Acad. Sci. U.S.A.* **2015**, *112*, 3686–3691.
[9] a) J. M. Guisan, G. Fernandez-Lorente, J. Rocha-Martin, D. Moreno-Gamero, *Curr. Opin. Green Sustainable Chem.* **2022**, *35*, 100593; b) R. A. Sheldon, A. Basso, D. Brady, *Chem. Soc. Rev.* **2021**, *50*, 5850–5862; c) J. M. Bolivar, J. M. Woodley, R. Fernandez-Lafuente, *Chem. Soc. Rev.* **2022**, *51*, 6251–6290; d) A. Basso, S. Serban, *Mol. Catal.* **2019**, *479*, 110607.
[10] a) H. J. Federsel, T. S. Moody, S. J. C. Taylor, *Molecules* **2021**, *26*, 2822; b) A. Liese, L. Hilterhaus, *Chem. Soc. Rev.* **2013**, *42*, 6236–6249.
[11] B. O. Burek, A. W. H. Dawood, F. Hollmann, A. Liese, D. Holtmann, *Front. Catal.* **2022**, *2*, 858706.
[12] P. De Santis, N. Petrovai, L.-E. Meyer, M. Hobisch, S. Kara, *Front. Chem.* **2022**, *10*, 985997.
[13] a) L.-E. Meyer, B. Fogtmann Hauge, T. Müller Kvorning, P. De Santis, S. Kara, *Catal. Sci. Technol.* **2022**, *12*, 6473–6485; b) M. Hobisch, P. De Santis, S. Serban, A. Basso, E. Byström, S. Kara, *Org. Process Res. Dev.* **2022**, *26*, 2761–2765.
[14] a) S. Bormann, D. Hertweck, S. Schneider, J. Z. Bloh, R. Ulber, A. C. Spiess, D. Holtmann, *Biotechnol. Bioeng.* **2021**, *118*, 7–16; b) W. Zhang, B. O. Burek, E. Fernandez-Fueyo, M. Alcalde, J. Z. Bloh, F. Hollmann, *Angew. Chem. Int. Ed.* **2017**, *56*, 15451–15455; c) Y. Shiraishi, S. Kanazawa, D. Tsukamoto, A. Shiro, Y. Sugano, T. Hirai, *ACS Catal.* **2013**, *3*, 2222–2227; d) A. Torres-Pinto, M. J. Sampaio, C. G. Silva, J. L. Faria, A. M. T. Silva, *Catalysts* **2019**, *9*, 990–1014.
[15] a) L. Schmermund, V. Jurkaš, F. F. Özgen, G. D. Barone, H. C. Büchsenschütz, C. K. Winkler, S. Schmidt, R. Kourist, W. Kroutil, *ACS Catal.* **2019**, *9*, 4115–4144; b) C. J. Seel, T. Gulder, *ChemBioChem* **2019**, *20*, 1871–1897.
[16] a) M. M. C. H. van Schie, W. Zhang, F. Tieves, D. S. Choi, C. B. Park, B. O. Burek, J. Z. Bloh, I. W. C. E. Arends, C. E. Paul, M. Alcalde, F. Hollmann, *ACS Catal.* **2019**, *9*, 7409–7417; b) J. Kim, S. H. Lee, F. Tieves, D. S. Choi, F. Hollmann, C. E. Paul, C. B. Park, *Angew. Chem. Int. Ed.* **2018**, *57*, 13825–13828; c) E. Churakova, M. Kluge, R. Ullrich, I. Arends, M. Hofrichter, F. Hollmann, *Angew. Chem. Int. Ed.* **2011**, *50*, 10716–10719.
[17] B. O. Burek, S. R. D. Boer, F. Tieves, W. Zhang, M. V. Schie, S. Bormann, M. Alcalde, D. Holtmann, F. Hollmann, D. W. Bahnemann, J. Z. Bloh, *ChemCatChem.* **2019**, *11*, 3093–3100.
[18] X. Deng, X. Zheng, F. Jia, C. Cao, H. Song, Y. Jiang, Y. Liu, G. Liu, S. Li, L. Wang, *Appl. Catal. B* **2023**, *330*, 122622.
[19] G. Moon, M. Fujitsuka, S. Kim, T. Majima, X. Wang, W. Choi, *ACS Catal.* **2017**, *7*, 2886–2895.
[20] L. Schmermund, S. Reischauer, S. Bierbaumer, C. K. Winkler, A. Diaz-Rodriguez, L. J. Edwards, S. Kara, T. Mielke, J. Cartwright, G. Grogan, B. Pieber, W. Kroutil, *Angew. Chem. Int. Ed.* **2021**, *60*, 6965–6969.
[21] B. O. Burek, D. W. Bahnemann, J. Z. Bloh, *ACS Catal.* **2018**, *9*, 25–37.
[22] a) C. Wang, R. Yan, M. Cai, Y. Liu, S. Li, *Appl. Surf. Sci.* **2023**, *610*, 155346; b) S. Li, M. Cai, Y. Liu, C. Wang, R. Yan, X. Chen, *Adv. Powder Mater.* **2023**, *2*, 100073.
[23] M. Hobisch, S. Kara, *Biorxiv* **2021**, DOI: 10.1101/2021.07.29.454275.
[24] B. S. Antharavally, K. A. Mallia, P. Rangaraj, P. Haney, P. A. Bell, *Anal. Biochem.* **2009**, *385*, 342–345.

Revised manuscript received: June 22, 2023
Accepted manuscript online: June 25, 2023
Version of record online: ■■, ■■

RESEARCH ARTICLE

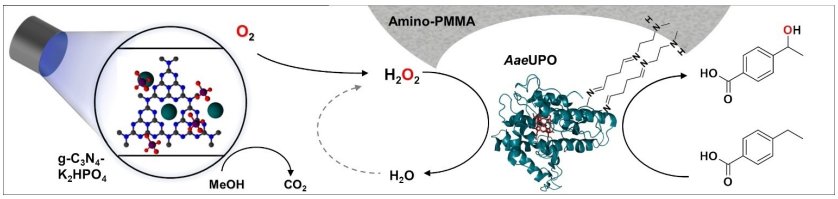

The right light for peroxizymes: Increased stability of peroxygenases can be achieved by a combination of enzyme immobilization and photocatalytic in situ hydrogen peroxide supply. Therefore, oxygen reduction over illuminated potassium phosphate-doped graphitic carbon nitride was cascaded with the unspecific peroxygenase from *Agrocybe aegerita* immobilized on an amino methacrylate carrier to hydroxylate 4-ethylbenzoic acid.

P. De Santis, D. Wegstein, Dr. B. O. Burek, J. Patzsch, Prof. Dr. M. Alcalde, Prof. Dr. W. Kroutil, Dr. J. Z. Bloh*, Prof. Dr. S. Kara**